



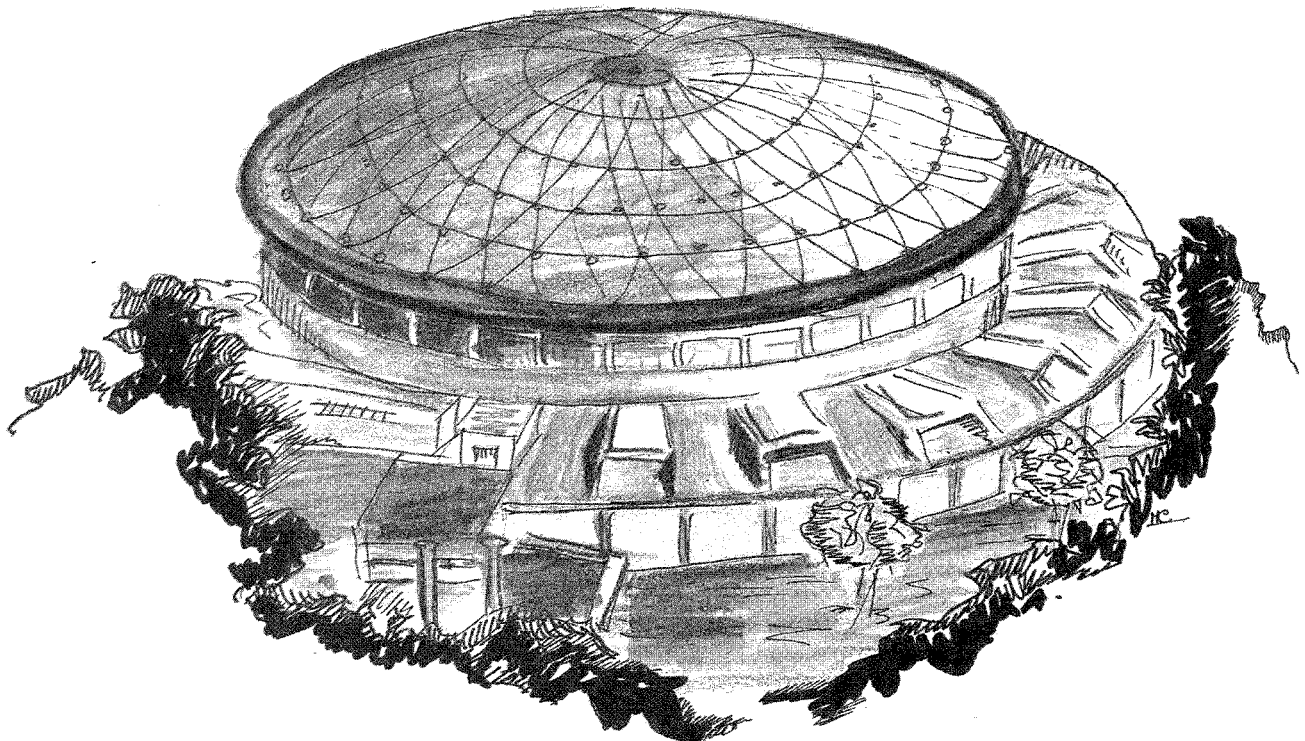
ISTITUTO NAZIONALE DI FISICA NUCLEARE - ISTITUTO NAZIONALE DI FISICA NUCLEARE - ISTITUTO NAZIONALE DI FISICA NUCLEARE - ISTITUTO NAZIONALE DI FISICA NUCLEARE

Laboratori Nazionali di Frascati

LNF-89/018(R)
27 Aprile 1989

R. Boni, A. Savoia, B. Spataro, F. Tazzioli, P. Fabbricatore, R. Parodi, P. Fernandes:

RF TEST OF A 6 GHz SUPERCONDUCTING CAVITY AT LNF



Servizio Documentazione
dei Laboratori Nazionali di Frascati
P.O. Box, 13 - 00044 Frascati (Italy)

LNF-89/018(R)
27 Aprile 1989

RF TEST OF A 6 GHz SUPERCONDUCTING CAVITY AT LNF

R. Boni, A. Savoia, B. Spataro, F. Tazzioli
INFN - Laboratori Nazionali di Frascati - Via E. Fermi 40, Frascati (Italy)

P. Fabbricatore, R. Parodi
INFN - Sezione di Genova - Via Dodecaneso 33, Genova (Italy)

P. Fernandes
CNR - Istituto di Matematica Applicata - Via L.B. Alberti 4, Genova (Italy)

ABSTRACT

RF tests of a 6 GHz Superconducting Cavity made of bulk niobium and working in a high order transverse electric mode (TE_{118}), have been carried out at LNF to measure the maximum achievable RF fields and to investigate the possibility of using it as a microwave undulator. The results obtained in this work and the experience gained in the field of Superconducting Radiofrequency are reported in this paper.

1. - INTRODUCTION

In 1988, the cryogenics and radiofrequency tests of a small cavity resonator made of bulk niobium have been carried out at LNF. The resonator had been particularly designed to behave as a microwave undulator as reported elsewhere^{1,2,3}. In a microwave cavity undulator the e.m. fields cause the particle to follow an undulated trajectory around the axis of the cavity.

The parameters that characterize a microwave cavity undulator are the quality factor Q_0 and the amplitude of the e.m. fields on the cavity axis, which is related to the maximum fields attainable on the surface of the cavity.

The relation between the factor Q_0 and the RF power P_D dissipated on the inner surface of the cavity is:

$$Q_0 = \frac{2\pi (\text{stored energy})}{\text{Energy lost per cycle}} = \frac{\omega U}{P_D} \quad (1)$$

In a microwave cavity undulator the fields are orthogonal to the average particle trajectory (see Fig. 1) and the usual concept of shunt-impedance, which is valid for accelerating cavities, is meaningless. The significant factor for an undulator is the parameter K:

$$K = \frac{e\lambda_0 B_0}{2\pi m c^2} \quad (2)$$

which is proportional to the peak magnetic field.

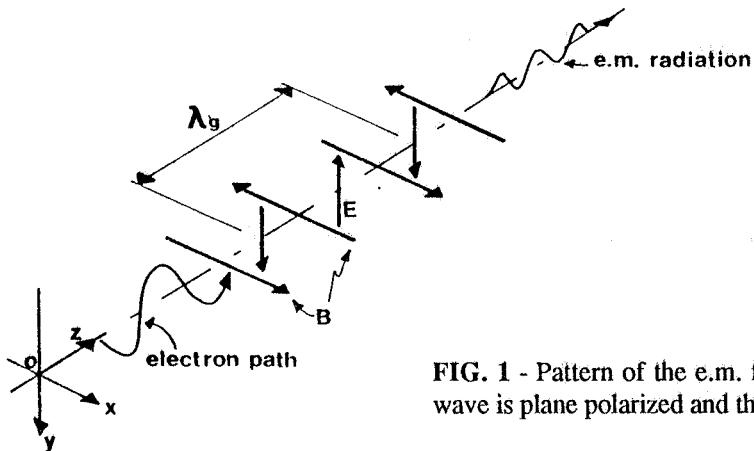


FIG. 1 - Pattern of the e.m. fields in the microwave undulator. The wave is plane polarized and the electrons undulate in the YZ plane.

The factors limiting the peak surface field are more severe in a superconducting (SC) cavity than in a normal one. In fact field emission loading can cause a SC cavity to quench at intensities that are usually tolerated by normal cavities.

Moreover, there is a critical magnetic field value which cannot be exceeded because a transition to normal state take place. At 6 GHz and 1.8 K the maximum achievable magnetic field has been estimated⁴ to be 1 kG with Niobium of residual resistance ratio (RRR) ≈ 60 . The value of the working frequency has been choosen as a compromise between a desired small undulator wavelength and a lower limit on the diameter of the beam access holes.

Computer codes like URMEL⁵, SUPERFISH⁶ or OSCAR2D⁷ are widely used for the calculation of the most important parameters of the cavity resonators to be used in particle accelerators or for other purposes. The code OSCAR2D has been successfully used in our case.

The test cavity is a waveguide shorted at the ends with two plates. The section of the cavity is elliptical to force a linear polarization of the RF fields and to avoid the ambiguity of the degeneration of TE₁₁ modes when the cross section is circular (modes having the same frequency but different configurations). The transverse electromagnetic fields (TE₁₁₈) cause the particle

beam to follow an undulated trajectory in a plane vertical to the magnetic field. For a careful study of the particle motion we refer to other articles^{1,3,8}.

The eccentricity given to the cavity cross section splits the frequency of the two orthogonal TE₁₁₈ modes by about 134 MHz. In this case we denote the modes by the subscripts "s" or "p" as shown in Table 1 which summarizes the most important characteristics of some resonances whose frequency is close to the frequency of TE_{118p} (second row of Table I) which is the investigated mode.

TABLE - I

| mode | fc(MHz) | fo(MHz) | n | H _T (G) | Q _o (10 ⁹) | P (mW) |
|-------|---------|---------|---|--------------------|-----------------------------------|--------|
| TE11s | 1770 | 5851 | 8 | 19.0 | 5.42 | 6.77 |
| TE11p | 2172 | 5985 | 8 | 27.0 | 6.19 | 6.07 |
| TM01s | 2593 | 6151 | 8 | 24.5 | 3.89 | 10.9 |
| TE12s | 2993 | 5725 | 7 | 25.8 | 4.44 | 8.09 |
| TE21p | 3280 | 5880 | 7 | 22.6 | 3.91 | 9.40 |
| TE12p | 3709 | 6130 | 7 | 27.0 | 4.56 | 8.40 |
| TM11s | 3894 | 6243 | 7 | 31.9 | 3.90 | 10.0 |
| TM11p | 4347 | 6033 | 6 | 35.6 | 3.51 | 10.8 |
| TE31s | 4382 | 6058 | 6 | 20.5 | 3.16 | 12.0 |
| TE31p | 4433 | 6095 | 6 | 20.6 | 3.07 | 12.4 |
| TM22s | 5231 | 5928 | 4 | 32.6 | 3.81 | 9.76 |
| TE22s | 5479 | 5864 | 3 | 12.7 | 4.91 | 7.50 |
| TM21p | 5516 | 5899 | 3 | 30.7 | 3.63 | 10.2 |
| TE41s | 5572 | 5952 | 3 | 11.5 | 2.47 | 15.0 |
| TE41p | 5587 | 5966 | 3 | 11.5 | 2.42 | 15.5 |

The columns represent respectively:

- f_c = cut-off frequency of the given mode below which the RF fields do not propagate in the waveguide having the same transverse section;
- f_o = resonant frequency;
- n = number of half periods of the electric field along the cavity;
- H_T = value of the transverse surface magnetic field for an energy stored in the cavity: U = 1 mJoule;
- Q_o = unloaded quality factor at 1.8 K;
- P = RF input power for the given H_T.

The data of Table I have been calculated with the code OSCAR2D which also allows to plot the field flux lines of the resonant modes as shown in Fig. 2 for some of them.

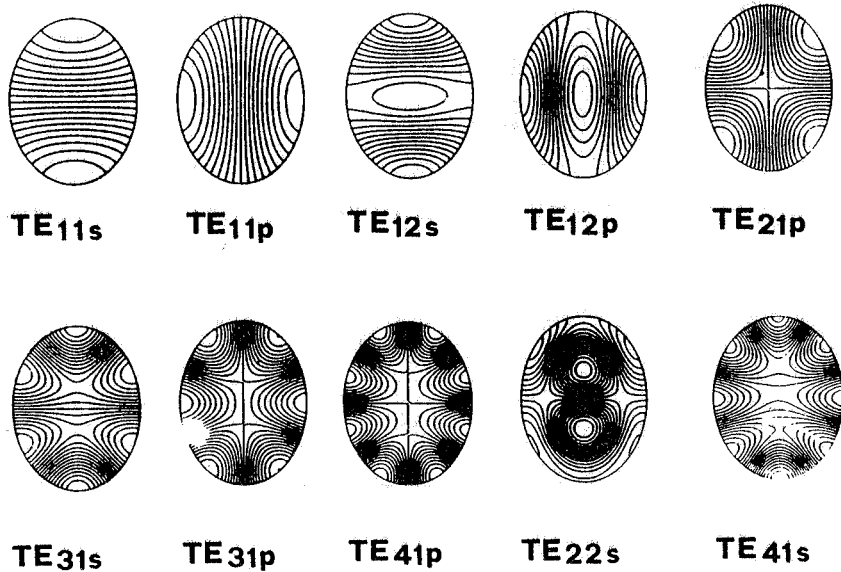


FIG. 2 - Electric field configurations ($r \cdot H\phi = \text{const.}$) for some TE resonant modes in the plane x-y of the cavity under test as calculated by the code OSCAR2D.

Additional important data for the structure under test and the investigated mode are given by the computer code OSCAR2D, for an energy stored inside the cavity $U = 1 \text{ mJoules}$:

$$E_{\max} = 0.45 \text{ MV/m} \quad \text{Surface electric field} \quad (3)$$

$$\frac{H_T(\text{gauss})}{\sqrt{P(\text{watt})} * Q_0} = \text{constant} = 4.4 * 10^{-3} \quad (4)$$

$$G = \omega \mu_0 \frac{\int_V H^2 dV}{\int_S H_{II}^2 dS} = Q_0 R_S = 1240 \Omega \quad \text{geometrical constant of the cavity} \quad (5)$$

where R_S is the surface resistance of the cavity metal.

The equation (4) is used to calculate the transverse magnetic field once one has measured the input RF power and the unloaded quality factor Q_0 .

For a SC material of transition temperature T_c and for frequencies up to about 10 GHz^{9,10} one has:

$$R_S = R_{\text{RES}} + A \frac{\omega^2}{T} \exp - \left(\alpha \frac{T_c}{T} \right) \quad \text{surface resistance} \quad (6)$$

where R_{RES} is the residual resistance of the surface and the second term is the R_{BCS} resistance based on the BCS theory⁹.

For Niobium one has:

$$A \approx 1.13 \cdot 10^{-24}, \quad \alpha \approx 1.76 \quad \text{and} \quad T_c = 9.25 \text{ K.}$$

R_{res} is independent of the temperature and essentially originates from the impurities on inner surface but also from the frozen-in Earth's magnetic field. Therefore, to have a low value of R_{res} a very careful cleaning treatment of the cavity and also magnetic shielding with μ -metal are required. R_{BCS} given by (6) is in good agreement with the experimental data obtained elsewhere^{11,12}.

2. - CAVITY DESIGN AND SURFACE CLEANING

The TE₁₁₈ cavity is shown in Fig. 3. It is made of bulk niobium of standard reactor grade (RRR = 68) and consists of a 215 mm long by 80x100 mm elliptical cylinder with two shorting endplates. The eccentricity of the cross section forces the polarization of the mode in the required direction (y axis).

A small feeding loop ($\approx 3 \times 3 \text{ mm}^2$) is located in a small cylinder welded on an endplate and its plane position is perpendicular to the magnetic field of the mode to be excited (TE₁₁₈), in order to couple with it as easily as possible. The loop can be moved inside the small cylinder allowing the adjustment of the coupling between the microwave amplifier and the resonator. The RF signal is detected with a probe placed on the other endplate and very weakly coupled with the RF fields.

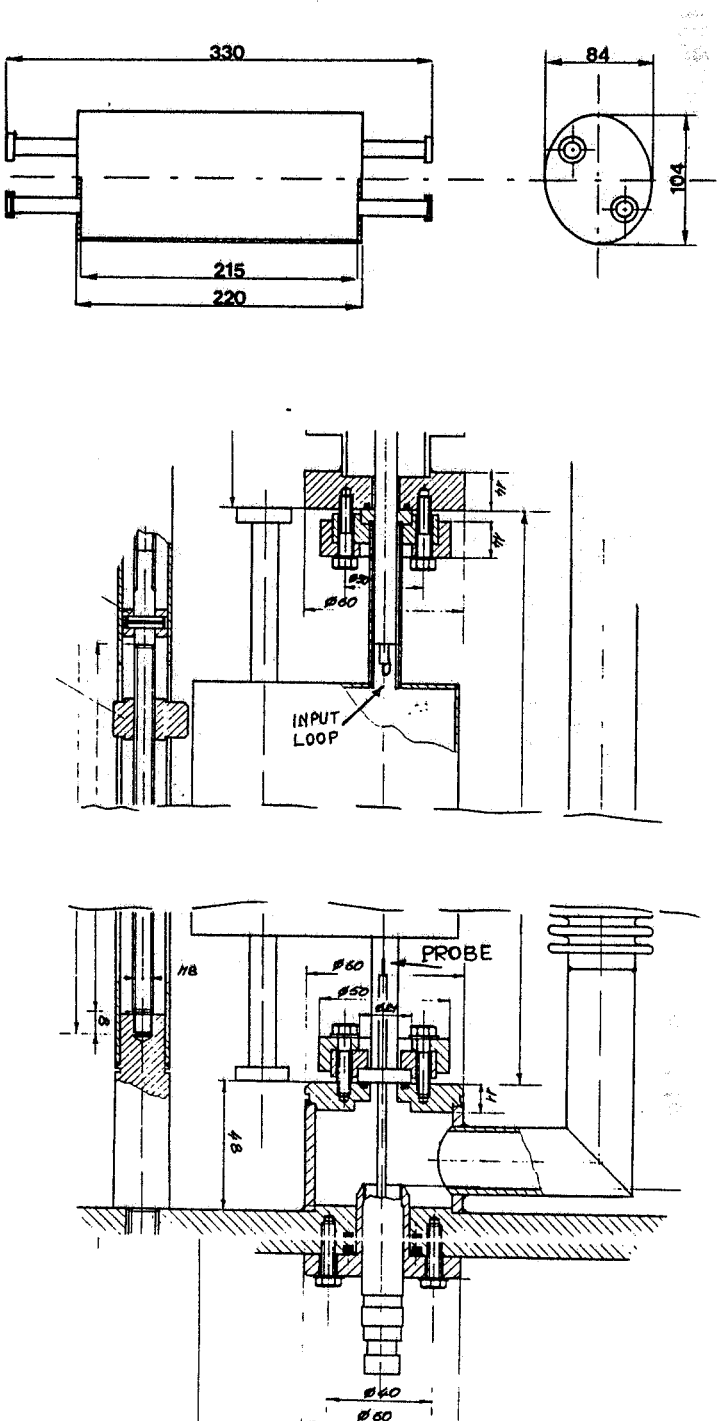
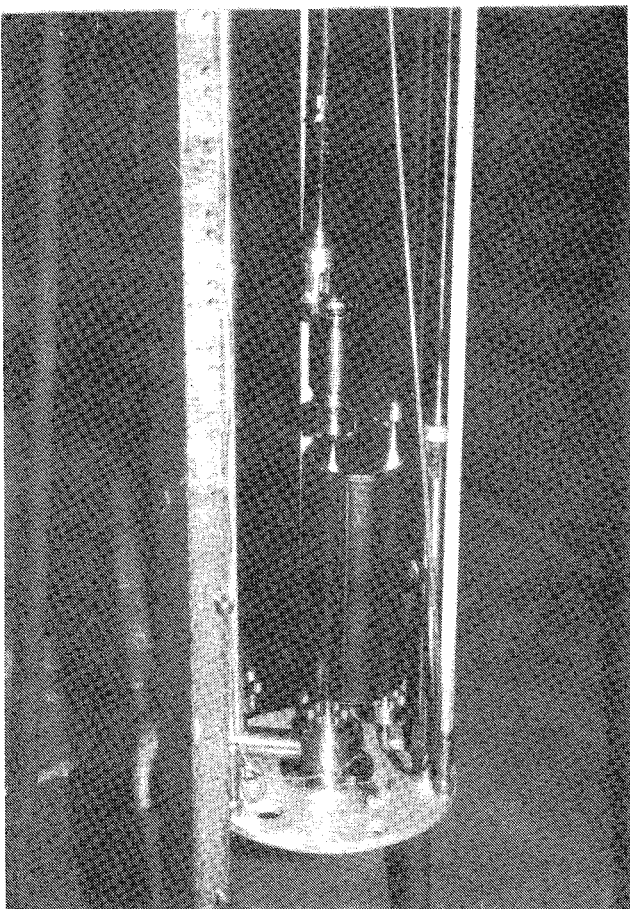


FIG. 3 - The resonator under test and the details of the coupling loop and pick-up probe.

The parts of the cavity were assembled with the electron beam welding (EBW) technique. A chemical polishing (CP)¹³ with a solution of equal volume of fluoric, nitric and phosphoric acid has been done at LNF followed by a rinsing with bi-distilled water and methilal. As noted above, the purpose of the cleaning treatment is to obtain the lowest possible R_{res} and therefore higher RF fields, higher Q-values and little electron emission.



The cavity was then vertically mounted in the cryostat (see Fig. 4) with the internal surface still wet and soon pumped at room temperature down to less than 10^{-8} Torr via an additional tube welded on its lower endplate. Several sheets of μ -metal 1 mm thick were wound around the cryostat for shielding the cavity from the Earth's magnetic field. A residual field of about 30 mGauss was measured inside the cryostat which is a commercial vertical dewar.

FIG. 4 - Mounting the S.C. in the cryostat.

3. - THE MICROWAVE MEASURING SET-UP

The SC is powered in pulsed mode allowing the measurement of the decay time of the RF energy stored in the resonator and hence the quality factor Q_o.

The microwave generator is a 2.3 - 13 GHz HP8683D and the power amplifier is a TWT Hughes mod.1277H02 with a gain of 30 dB in the range 4 - 8 GHz. The microwave power available at the cavity input is 10 watts. The auxiliary instrumentation consists of a HP8562A spectrum analyzer and a HP436A power meter.

Since the very narrow bandwidth of a SC, an accurate tuning system is needed to keep the cavity in resonance when dissipating the RF power. In our case, we do not mechanically deform the cavity shape but, for simplicity, a feedback loop causes the frequency of the microwave generator to change according to the variations of the resonant cavity frequency. A double-

balanced mixer (Anzac MDC-186), used as phase discriminator, provides a signal error which feeds the Phase-Lock input of the generator by means of a suitable RC network and keeps the SC cavity in resonance. Fig. 5 shows the schematic layout of the microwave circuit evidencing the feedback loop for the automatic tuning.

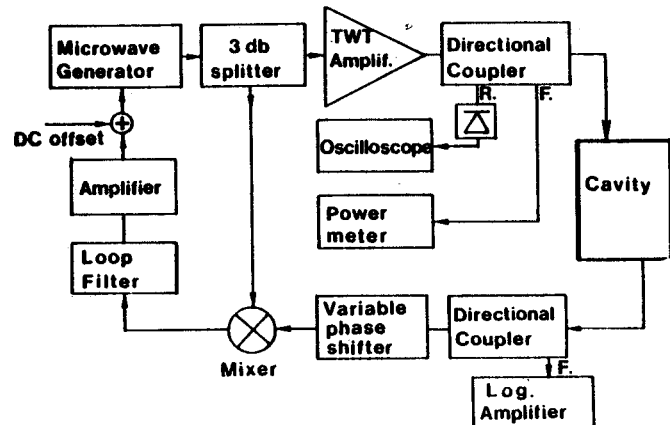


FIG. 5 - The microwave measuring set-up.

The L.O. input of the mixer is fed with a constant RF level of + 7dBm via a 3 dB coupler from the generator. This guarantees the best performances of the mixer. The RF level is adjusted with a variable attenuator connected at the power amplifier input. A phase shifter, connected to the RF terminal of the mixer, introduces a variable delay in the loop to select the best operating point of the feedback. The connections between the components of the circuit are made with RG-141/U and RG-213 cables using SMA and N connectors instead of standard waveguides WR159 or WR137. This solution is less expensive and allows greater flexibility during the measurements even though it causes larger power losses.

The RF circuit provides three check-points of the microwave signals. The power reflected from the cavity is monitored on an oscilloscope by sampling it with a 20 dB Directional Coupler (D.C.) and the incident power is also sampled with an additional 20 dB D.C. and measured with the power meter; the RF signal, which is transmitted out the cavity through the pick-up probe, is detected with a 10 dB D.C. and displayed on the spectrum analyzer in logarithmic scale.

4. - RF MEASUREMENTS OF THE 6 GHz CAVITY RESONATOR

The resonant frequency of the TE₁₁₈ mode measured at 4.2 K is 6,010 MHz, about 25 MHz higher than that calculated with the computer code. The variation is partly due to the thermal contraction of Niobium during the "cool-down" and partly to the mechanical tolerances. At 1.3 K the frequency is a little lower than at 4.2 K because when the Helium bath is pumped to decrease the temperature, the cavity slightly expands.

For an easier calculation of Q_0 , the cavity has been fed at matched coupling ($\beta=1$), for any operating temperature, by adjusting the position of the input loop. In these conditions the power reflected by the cavity vanishes and its time behaviour is shown in Fig. 6 at 4.2 K for an input RF power of 1 W. Fig. 7 presents the related transmitted signal as displayed by the spectrum analyzer in logarithmic scale. In this case, the RF energy has a decay of about 30 dB in 6 msec. corresponding to an unloaded quality factor given by the following expression which is derived in appendix 1:

$$Q_0 = (1 + \beta) * 4.34 \omega \frac{\Delta T}{\Delta \text{dB}} \approx 6.5 * 10^7 \quad (7)$$

The transverse RF magnetic field, calculated with (4) is ≈ 35 Gauss.

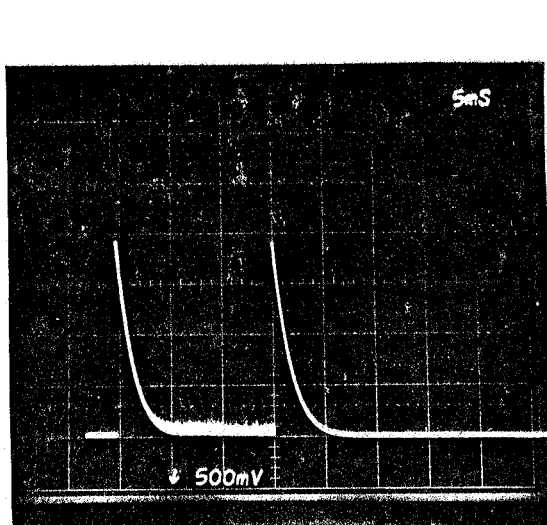


FIG. 6 - Time behaviour of the reflected power for a matched coupling.

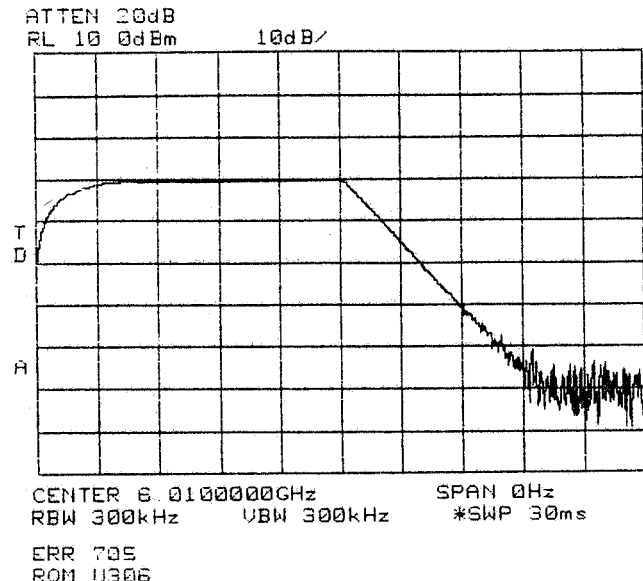


FIG. 7 - Sample of RF signal monitored by the pick-up probe.

We have done several measurements at 4.2 K and 1.3 K, before and after C.P. treatments and He-processing which is a well known procedure for improving the smoothness of the internal surfaces.

In Figs. 8 and 9 the dependence of the quality factor Q_0 on the transverse surface magnetic field at the endplates of the SC is presented at 4.2K and 1.3K respectively. The improvements of Q_0 due to repeated C.P. treatments and He-processing are clearly shown.

Figures 10 through 12 show some waveforms of RF signals.

Using equation (5) and the experimental data, one can obtain the diagram of Fig. 13 where the surface resistance R_s of the Niobium under test is plotted versus the ratio T_c/T .

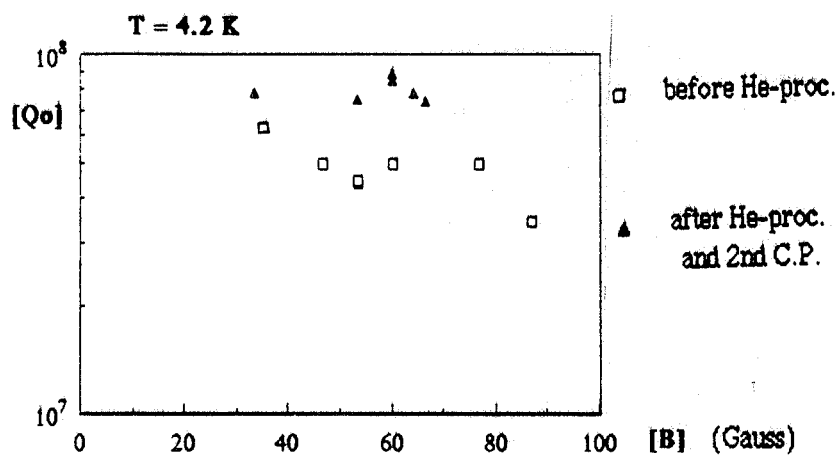


FIG. 8 - The factor Q_o versus B at 4.2 K.

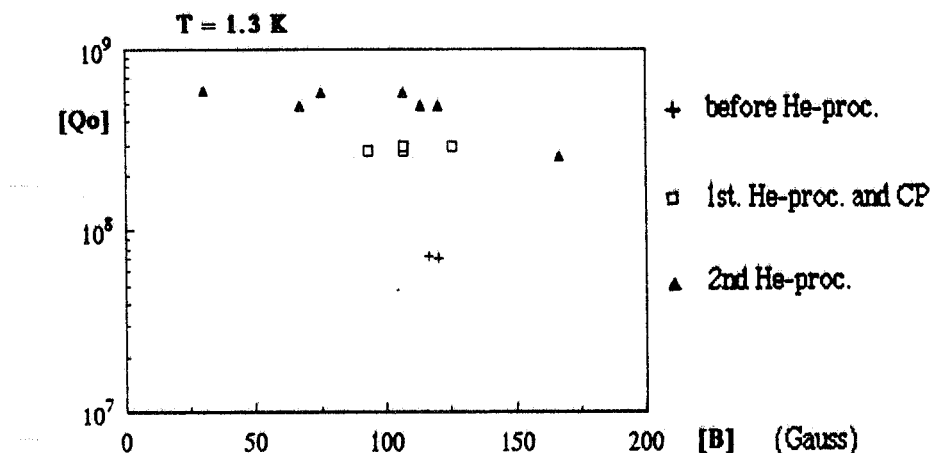


FIG. 9 - The factor Q_o versus B at 1.3 K.

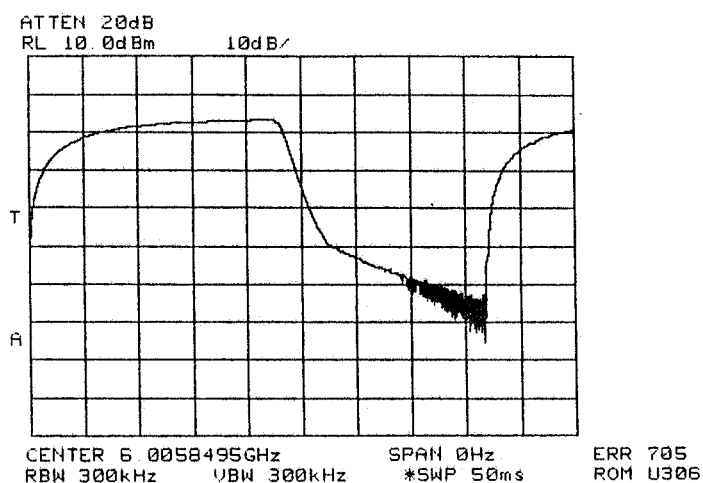


FIG.10 - Waveform of a RF cavity pulse evidencing a degradation of Q due to high fields; $P_i \approx 6 \text{ W}$; $T = 2.1 \text{ K}$; $B \approx 180 \text{ G}$.

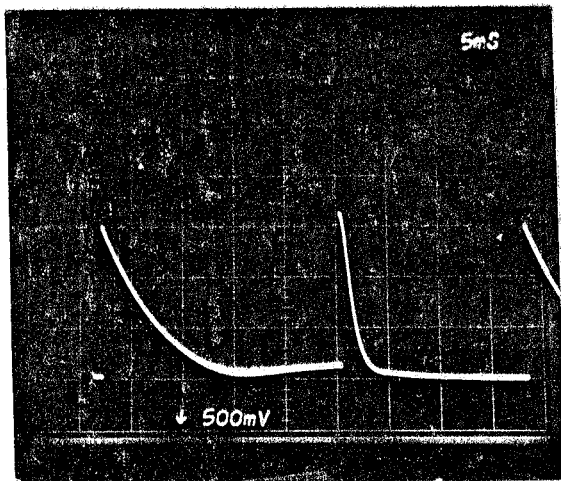


FIG.11 - Time behaviour of the reverse power for the pulse of Fig. 10

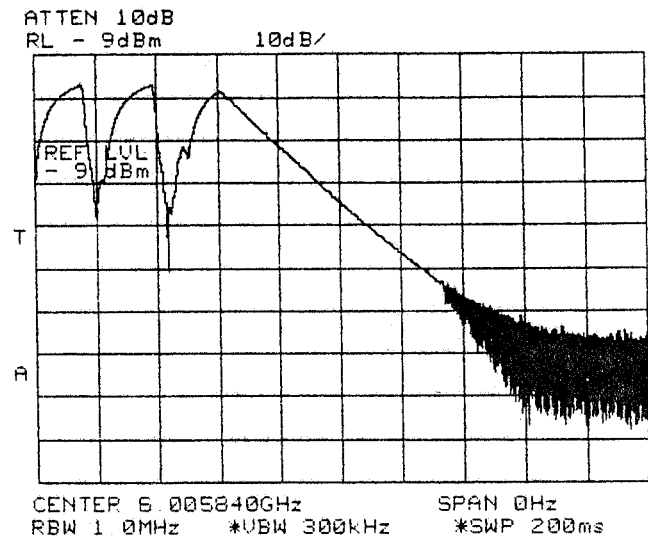


FIG.12 - An example of "quench" during He-processing.

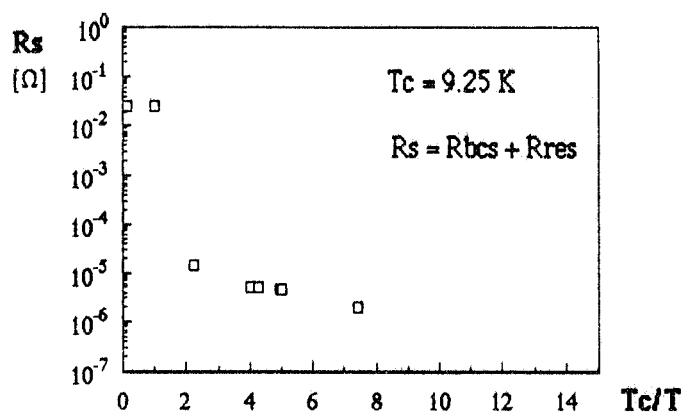


FIG.13 - Surface resistance of the 6 GHz Nb cavity.

The curve in Fig. 13 tends to saturate for a value of R_s which represents the residual resistance of the internal Niobium surface.

In appendix 2 the value of the residual resistance R_{res} is calculated. It results to be rather high ($\approx 2 \mu\Omega$ instead of $< 200 - 300 \text{ n}\Omega$).

The reason of this value could be due to an insufficient C.P. treatment or to inadequate internal surface smoothness of the weldings. Nevertheless, magnetic fields in excess of 150 Gauss with Q_0 factors of some 10^8 have been measured at 1.3 K (see Fig. 9). The ratio (E_{max}/B_{max}) as

given by the computer code OSCAR2D is about 1.7×10^4 with B_{\max} in Gauss. Therefore the corresponding surface electric field is nearly 2.6 - 2.8 MV/m.

In Table II we summarize the most important parameters of the superconducting cavity and the results obtained during the tests.

TABLE - II

| | |
|--|---|
| Mode of operation | TE ₁₁₈ |
| Calculated resonant frequency | F _c = 5985 MHz |
| Measured resonant frequency at 4.2 K | F _{o1} = 6010 MHz |
| Measured resonant frequency at 1.3 K | F _{o2} = 6006 MHz |
| Max. unloaded Q at 4.2 K | Q _{o1} = 8.8×10^7 |
| Max. unloaded Q at 1.3 K | Q _{o2} = 6×10^8 |
| Max. transverse magnetic field at 1.3 K <i>(limited by the available RF power)</i> | H _T = 170 Gauss |
| Max. surface electric field at 1.3 K | E _T = 2.9 MV/m |
| Probe coupling at 4.2 K | $\beta_{P1} = 2.5 \times 10^{-4}$ |
| Probe external Q at 4.2 K | Q _{extp1} = 3.5×10^{11} |
| Probe coupling at 1.3 K | $\beta_{P2} = 8 \times 10^{-4}$ |
| Probe external Q at 1.3 K | Q _{extp2} = 7.5×10^{11} |

5. - CONCLUSIONS

A 6 GHz Superconducting Cavity resonator made of bulk niobium has been tested at LNF. The maximum obtainable field was limited by the available RF power. With a better treatment of the cavity surface and a more accurate electron beam welding, a quality factor greater than 10^9 could certainly be reached, approaching, with about 10 W of RF power, the maximum achievable RF magnetic fields that are estimated to be ≈ 1 kG for bulk Niobium of RRR = 60 at 6 GHz and 1.8K.

ACKNOWLEDGEMENTS

The authors are indebted with those who greatly collaborated to this work. They are especially grateful to Dr. A. Gallo for designing the feedback loop and to P. Baldini, R. Bolli, F. Campolungo, M. Capozi, M. De Giorgi, F. Lucibello and S. Quaglia for their enthusiastic support. Special thanks are also due to S. Faini, R. Ceccarelli, A. Fiore and R. Lanzi for the assistance in cryogenics. This work has been supported by "gruppo V" of INFN.

APPENDIX 1

The expression of the quality factor Q_0 can be calculated from the power decay waveform.

From Fig. 14 one has:

$$P_1 = P_0 * e^{-\frac{t}{\tau}}$$

$$P_2 = P_0 * e^{-\frac{t'}{\tau}}$$

with τ = exponential time decay.

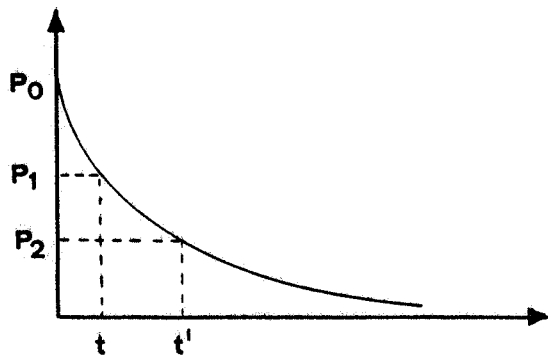


FIG. 14 - Power decay of a RF pulse

Then:

$$\frac{P_1}{P_0} = e^{-\frac{t}{\tau}} ; \frac{P_2}{P_0} = e^{-\frac{t'}{\tau}}$$

$$\frac{P_1}{P_0} - \frac{P_2}{P_0} = e^{-\left(\frac{t-t'}{\tau}\right)}$$

$$10 \log_{10} \left(\frac{P_1}{P_0} - \frac{P_2}{P_0} \right) = 10 \log_{10} \left[e^{-\left(\frac{t-t'}{\tau}\right)} \right] = - \frac{t-t'}{\tau} \log_{10} e$$

that is:

$$\Delta dB = - 4.34 * \frac{\Delta t}{\tau}$$

and taking:

$$Q_L = \omega \tau = \frac{Q_0}{(1+\beta)} \text{ loaded quality factor}$$

one has :

$$Q_0 = (1+\beta) * 4.34 \omega \frac{\Delta t}{\Delta dB}$$

APPENDIX 2

Experimentally, one finds:

$$R_S = R_{RES} + A \frac{\omega^2}{T} \exp - \left(\alpha \frac{T_c}{T} \right) = R_{RES} + R_{BCS} \quad \text{surface resist. of a S.C.}$$

and with $a = 1.76$, then:

$$\frac{R_{BCS}(4.2K)}{R_{BCS}(1.3K)} = \frac{\frac{1}{4.2} \exp \left[-1.76 * \frac{9.25}{4.2} \right]}{\frac{1}{1.3} \exp \left[-1.76 * \frac{9.25}{1.3} \right]} \approx 1760$$

Moreover:

$$\text{for } T_c = 4.2 \text{ K then } \dots Q_0 = 9 * 10^7 ; R_S = G/Q_0 = 1240 / 9 * 10^7 = 1.38 * 10^{-5} \Omega$$

$$\text{for } T_c = 1.3 \text{ K then } \dots Q_0 = 6 * 10^8 ; R_S = G/Q_0 = 1240 / 6 * 10^8 = 2 * 10^{-6} \Omega$$

$$R_S(1.3K) = R_{BCS}(1.3K) + R_{RES}$$

$$R_S(4.2K) = R_{BCS}(4.2K) + R_{RES}$$

$$R_{BCS}(1.3K) = \frac{1}{1760} * R_{BCS}(4.2K)$$

$$R_{BCS}(4.2K) = R_S(4.2K) - R_{RES}$$

and :

$$\begin{aligned} R_S(1.3K) &= \frac{1}{1760} * [R_S(4.2K) - R_{RES}] + R_{RES} = \\ &= \frac{1}{1760} * R_S(4.2K) + \left[1 - \frac{1}{1760} \right] * R_{RES} = \\ &= \frac{R_S(4.2K)}{1760} + 0.9994 * R_{RES} \end{aligned}$$

Finally :

$$R_{RES} = \left[R_S(1.3K) - \frac{1}{1760} * R_S(4.2K) \right] / 0.9994 \approx 2 * 10^{-6} \Omega$$

R_{BCS} can now be easily calculated :

$$R_{BCS}(4.2K) \approx 1.18 * 10^{-5} \Omega \quad \text{and} \quad R_{BCS}(1.3K) \approx 6.7 * 10^{-9} \Omega$$

REFERENCES

- (1) R. Boni, P. Fernandes, R. Parodi, A. Savoia, B. Spataro, F. Tazzioli, "Progetto di un Ondulatore Superconduttore a Microonde per la Generazione di Luce di Sincrotrone", Proc. of the 6th Riunione di Elettromagnetismo Applicato, Trieste, (Oct. 1986), 3.
- (2) R. Boni, P. Fabbricatore, P. Fernandes, U. Guerreschi, R. Parodi, F. Rosatelli, A. Savoia, B. Spataro, F. Tazzioli, "Design and test of a Superconducting Microwave Undulator for Short Wavelength Synchrotron Radiation Generation", Proc. of the 12th International Cryogenic Engineering Conference, Southampton, U.K., (July 1988), published by Butterworth and Co. Ltd, Surrey, UK.
- (3) R. Boni, P. Fabbricatore, P. Fernandes, R. Parodi, A. Savoia, B. Spataro, F. Tazzioli, "Superconducting Microwave Undulator", Review of Scientific Instruments, 1989, to be published.
- (4) P. Fernandes and R. Parodi, Cryogenics, Vol. 4, (Aug. 1984), 433.
- (5) T. Weiland, "URMEL User Guide", DESY, M-24 (1982).
- (6) K. Halbach and R. Holsinger, Particle Accelerator 7, (1976), 213.
- (7) P. Fernandes and R. Parodi, IEEE Trans. Magn. Mag-24, 154 (1988).
- (8) K. Batchelor, 1986 Linear Accelerator Conference Proceedings, SLAC 303, Stanford CA, (1986), 272.
- (9) D. Mattis and J. Bardeen, Phys. Rev. 111, (1958), 412.
- (10) J. Halbritter, Proc. of the Workshop on RF Superconductivity, KFK 3019, Karlsruhe, (1980), 190.
- (11) U. Klein, Dissertation, University of Wupperthal, WUB-DI, 81-2, (1981).
- (12) G. Muller, Dissertation, University of Wupperthal, WUB-DI, 83-1, (1983).
- (13) D. Bloess, Proc. of the Second Workshop on RF-Superconductivity, Geneva, Switzerland, (July 1984), 409.